

# ADAPTIVE FLOATING NODE METHOD FOR THE MODELLING OF DELAMINATION FRACTURE OF COMPOSITES

X. Lu<sup>1</sup>, B.Y. Chen<sup>2</sup>, V.B.C. Tan<sup>3</sup> and T.E. Tay<sup>4</sup>

<sup>1</sup> Department of Mechanical Engineering, National University of Singapore, 117576, Singapore, NUS, xinlu@u.nus.edu

<sup>2</sup> Institute of High Performance Computing, 138632, Singapore, IHPC, boyang.chen.cn@gmail.com

<sup>3</sup> Department of Mechanical Engineering, National University of Singapore, 117576, Singapore, NUS, mpetanbc@nus.edu.sg

<sup>4</sup> Department of Mechanical Engineering, National University of Singapore, 117576, Singapore, NUS, mpetayte@nus.edu.sg

**Keywords:** Progressive damage, Delamination analysis, Floating node method, Adaptive refinement, Numerical modelling

## ABSTRACT

The traditional cohesive element (CE) has been developed and widely employed to model the delamination and matrix cracking in composite materials. However, since it is based on the cohesive zone model (CZM), an extremely fine mesh along the potential crack path is required in order to achieve accurate predictions. Sufficient number of CEs must be embedded within the cohesive zone ahead of the crack tip or delamination front, resulting in prohibitively high computational cost for application to composite structures. To address this problem, an adaptive floating node method (A-FNM) is developed in this work. Element with adaptive partitioning capabilities is formulated and by transforming the element configurations adaptively, the localized refinement and coarsening schemes are applied on an originally coarse mesh. It is demonstrated that, without loss of accuracy, the present method greatly simplifies the modelling procedures and reduces the computational cost.

## 1 INTRODUCTION

Recently, an approach called the floating node method (FNM) for explicitly introducing discrete multiple cracks in finite elements (FE) for progressive damage modelling in laminated fibre-reinforced composites (FRC) has been proposed [1, 2]. It is particularly effective for modelling damage in cases involving strong and multiple interactions between evolving matrix cracks and delamination, where the smeared crack and material property degradation models do not always yield accurate results [3-5]. The FNM essentially seeds additional degrees of freedom (DOF) through “floating” nodes which are positioned in the FE mesh as the cracks, delamination or damage progress through the structure until final failure. Without remeshing the original FE model, the mesh near the advancing damage regions is progressively refined, driven by the mechanics and physics of the fracturing and damaging processes. This approach however, is computationally intensive because all the cracks are represented explicitly with cohesive elements and the element sizes must be kept smaller than the cohesive zone [6, 7].

In this study, an adaptive floating node method (A-FNM) which may potentially reduce model size and computational effort is proposed. In a growing damage region or advancing damage front, it is necessary for the mesh to be very fine; however, in the intact region and in the wake of the front within the damaged region, there is less need for the increased refinement. In the proposed A-FNM, elements with adaptive partitioning capabilities are designed such that a coarse overall mesh may be used and local refinement and coarsening may be applied within damaged elements only. Conceptually, this could be particularly useful in cases of advancing delamination or concentrated damage fronts. The proposed A-FNM element (Fig.1 (a)) may be formulated as a master element (b), a refined element (c) and a reverted element (d), depending on the progressive damage process, i.e. the adaptive refinement and coarsening scheme is implemented during the analysis. The implementation and application of the AFNM will be presented in the following chapters.

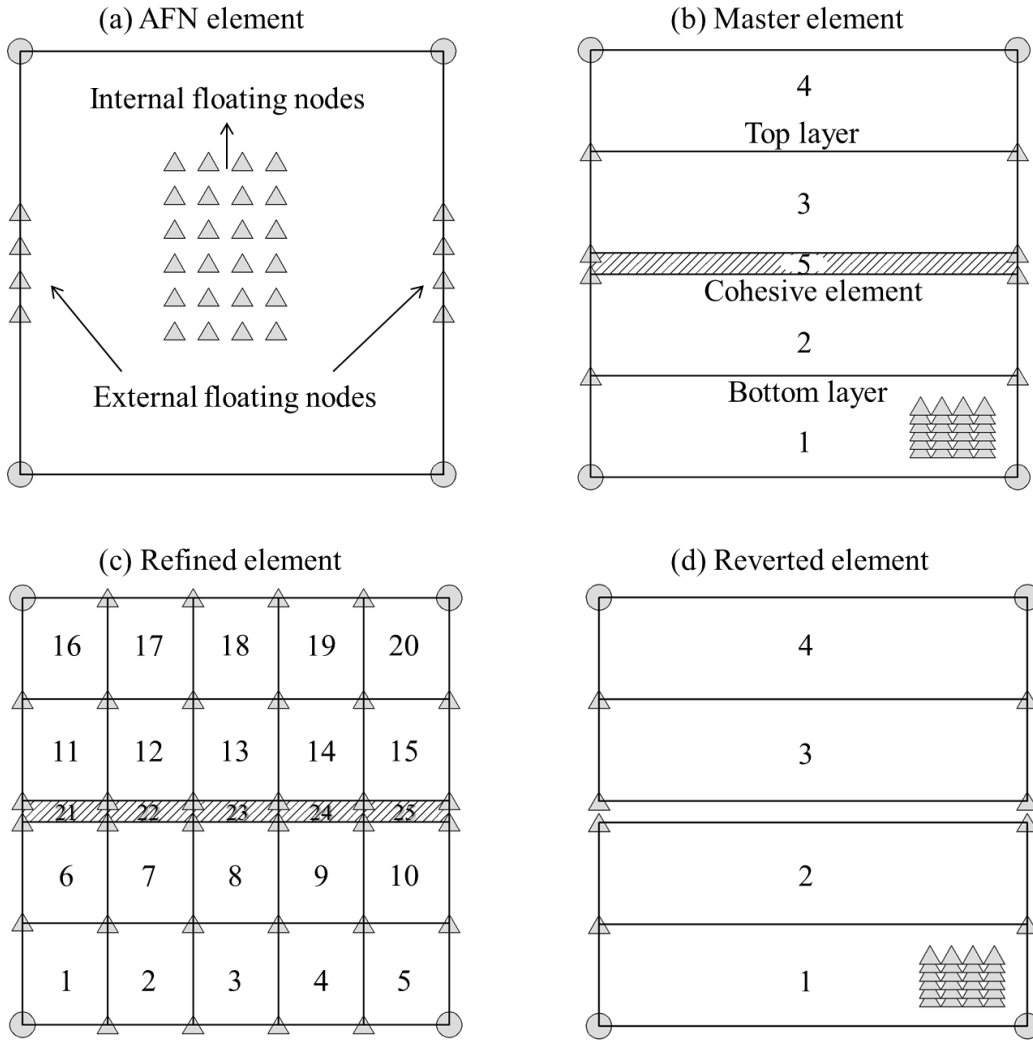


Figure 1: Element configurations.

## 2 ADAPTIVE FLOATING NODE METHOD (A-FNM)

The A-FNM as well as the refinement & coarsening schemes is illustrated by analysis of delamination growth in a double cantilever beam specimen. As shown in Fig. 2, the global nodal connectivity of the example is,

$$\begin{aligned}
 \text{I: } & \{1, 2, 7, 6, 11\sim 14, 15\sim 18, 31\sim 54\} \\
 \text{II: } & \{2, 3, 8, 7, 15\sim 18, 19\sim 22, 55\sim 78\} \\
 \text{III: } & \{3, 4, 9, 8, 19\sim 22, 23\sim 26, 79\sim 102\} \\
 \text{IV: } & \{4, 5, 10, 9, 23\sim 26, 27\sim 30, 103\sim 126\}
 \end{aligned} \tag{1}$$

This nodal connectivity will remain constant throughout the analysis when the refinement and coarsening schemes are performed, and hence the global successive remeshing and mapping operations are not required.

A refinement zone ahead of the crack tip is defined, such that all the elements within this refinement zone should be converted to the refined elements (Fig. 2). Physically, it defines a critical region in front of the crack tip, where stress gradient is very high and small size of CEs must be used to accurately capture the highly nonlinear material behaviors.

Since localized nonlinearity and intense stress variation ahead of the crack front is captured by the refined element configurations, the size of the sub elements should be sufficiently small. This length scale requirement is determined by the length of cohesive zone  $l_{CZ}$ , which can be estimated based on materials properties and loading conditions. For an accurate finite element modelling, it has been demonstrated that at least three CEs are required within the cohesive zone [6-8]. Hence, the size of the sub CEs in a refined element is given by,

$$l_{CE} = l_{CZ}/3 \quad (2)$$

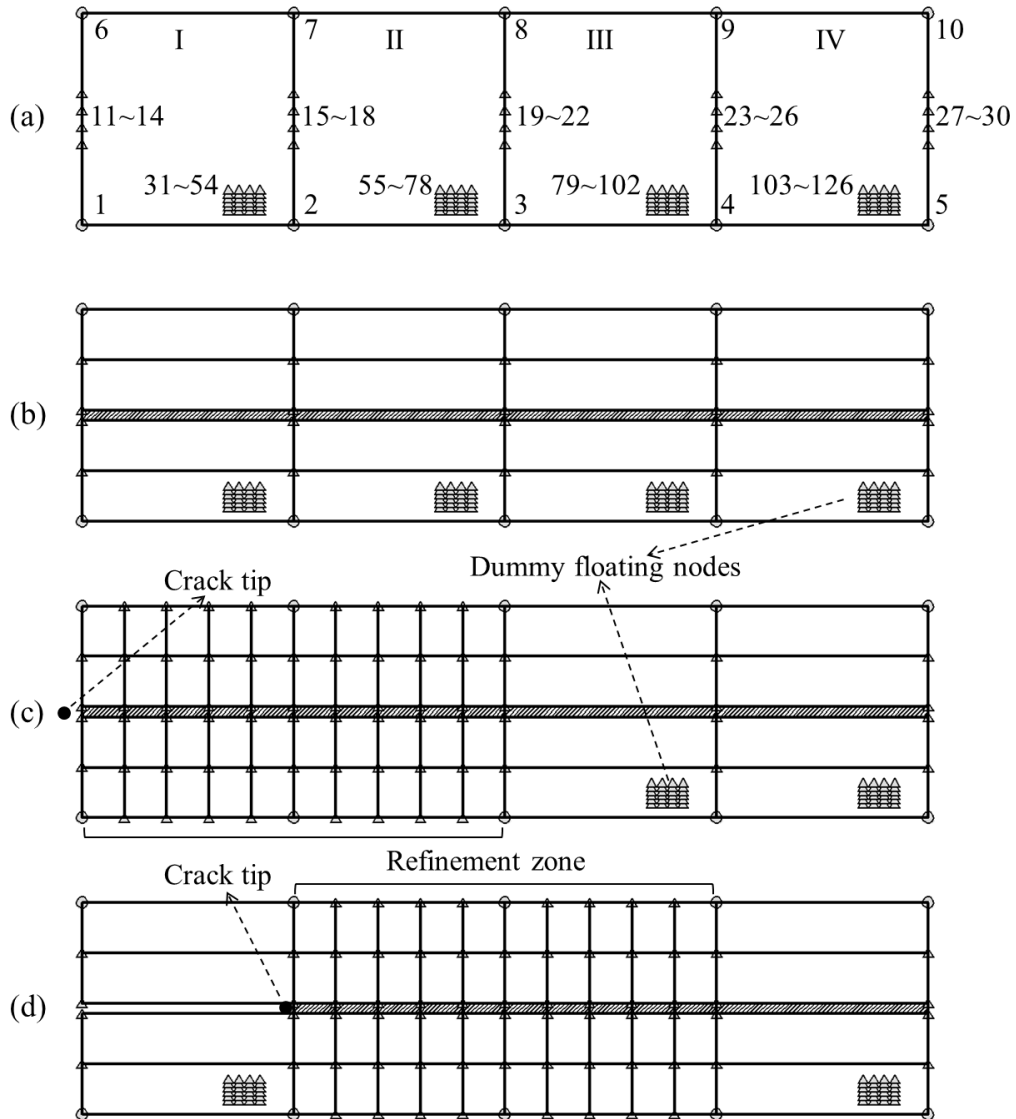


Figure 2: An example of A-FNM element modelling: (a) floating node numbering and global connectivity; (b) initial configuration with master elements; (c) refined elements in the refinement zone; (d) moving refinement zone within the mesh.

In this study, the length of the refinement zone,  $l_{rf}$ , is set to be three times the length of the cohesive zone,

$$l_{rf} = 3 \cdot l_{CZ} \quad (3)$$

According to the Fig. 3, which shows the normal traction vs. the distance ahead of the crack tip, the refinement zone given by Eq. (3) is able to cover the critical high-stress-gradient region and hence accurate predictions should be expected.

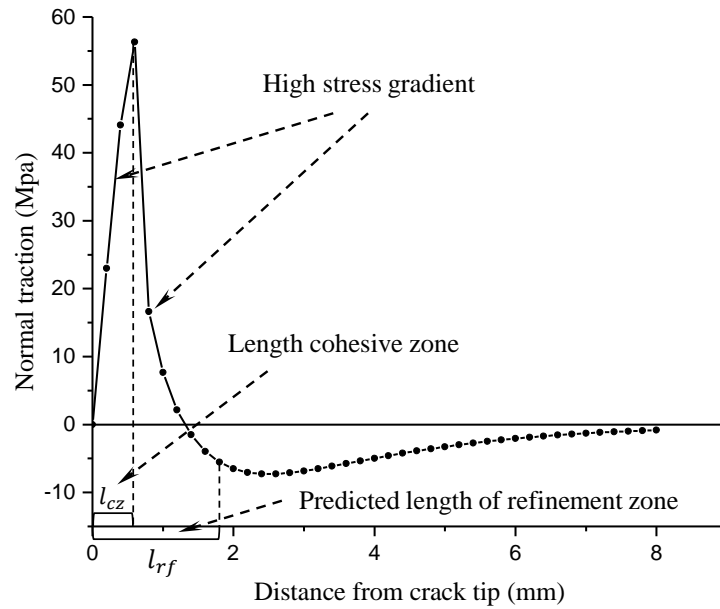


Figure 3: Normal traction vs. the distance ahead of the crack tip at the onset of delamination.

### 3 NUMERICAL VERIFICATIONS

In this section, the proposed A-FNM is applied to modelling the delamination failure of composite laminates. The adaptive floating node element (A-FNE) shown in Fig. 1 is implemented as a user-defined element (UEL) in in Abaqus software package (version 6.14). With such an A-FNE, interfacial delamination under mode-I, mode-II and mixed-mode loading can be easily simulated. To demonstrate the correctness and efficiency of the A-FNM, some representative numerical examples reported in the literature are studied in this section [9, 10]. The material properties for numerical analysis are listed in the Table 1.

	$E_{11}$ (GPa)	$E_{22}/E_{33}$ (GPa)	$G_{12}/G_{13}$ (GPa)	$G_{23}$ (GPa)	$\nu_{12}/\nu_{13}$ (-)	$G_{Ic}$ (N/mm)	$G_{IIc}$ (N/mm)	$\sigma_{max}/\tau_{max}$ (Mpa)	$\eta$ (-)
<b>DCB</b>	135.3	9	5.2	3.08	0.24	0.28	-	57	-
<b>ENF</b>	135.3	135.3	-	-	0.25	-	4	57	-
<b>MMB</b>	135.3	9	5.2	3.08	0.24	4	4	57	2

Table 1: Material properties used in section 3.

#### 3.1 Double cantilever beam (DCB) test: mode-I delamination

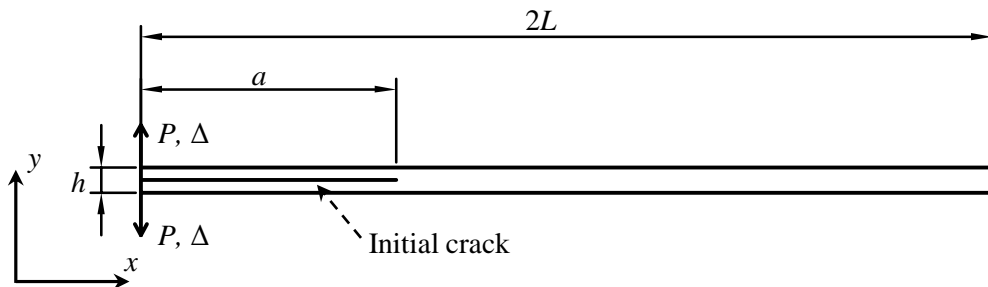


Figure 4: DCB test, set-up and loading conditions.

As shown in Fig. 4, a typical DCB problem illustrated in [10] is studied. The dimensions of the beam are length  $2L = 100\text{mm}$ , thickness  $h = 3\text{mm}$  and width  $20\text{mm}$ . An initial crack of length  $a = 30\text{mm}$  is embedded in the beam and the material properties adopted for this DCB tests are shown in Table 1. The crack is opened and propagates under the prescribed displacements  $\Delta$  at the endpoint of the embedded crack.

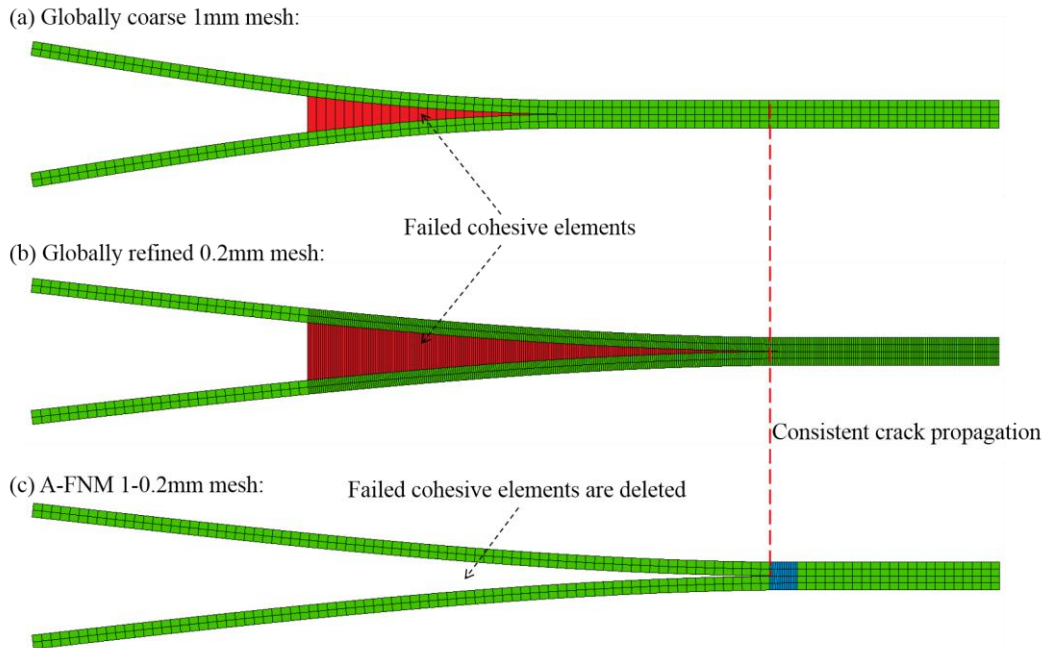


Figure 5: DCB test, comparison between traditional FEM models and A-FNM models.

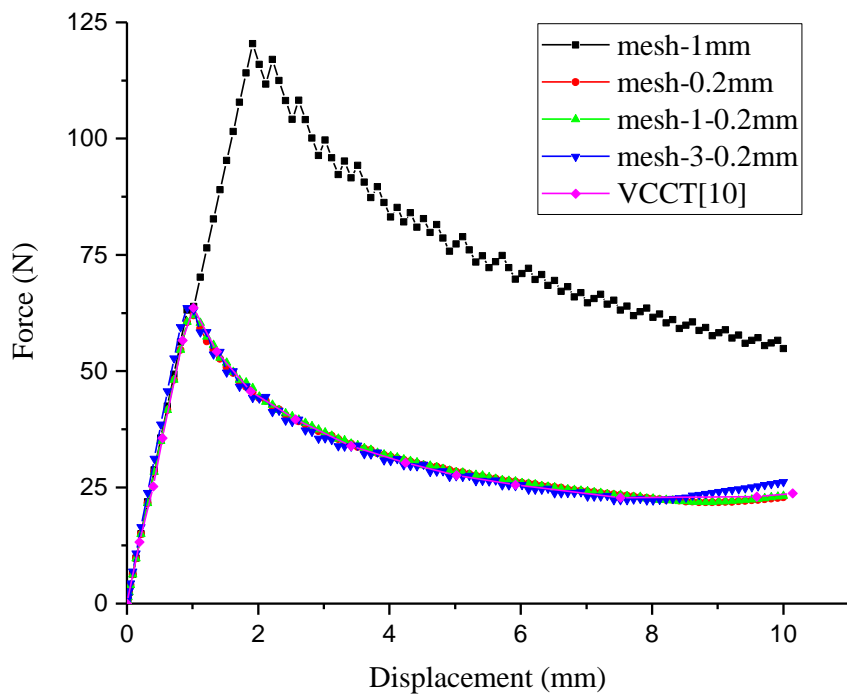


Figure 6: DCB test, comparison between traditional FEM models and A-FNM models.

Mesh size (mm)	0.2	AFN 1-0.2	AFN 3-0.2
Computational time (s)	640.58	368.82	336.71

Table 2: DCB test, computational cost for different models.

The comparison of the numerical results from different models are given in Fig. 5 and Fig. 6. As can be observed, the globally 1mm mesh is too coarse to correctly capture the onset and propagation of delamination, while globally refined 0.2mm mesh provides accurate predictions. If A-FNM is adopted, an adaptive 1-0.2mm mesh is applied in the FE analysis (Fig. 5c), and the local refinement zone will move consistently with the advancing crack front. In this case, the loading response as well as the predicted damage evolution shows good agreement with the results obtained from the globally refined model. Hence, accurate simulations are achieved using the A-FNM.

Furthermore, another case with 3-0.2mm mesh is also studied using the A-FNM. For this scenario, the original A-FNE mesh is 3mm, and the initial CE is divided into 15 sub-CEs in the refined configurations to meet the 0.2mm size requirement. Similarly, accurate prediction is expected as shown Fig. 6.

The computational cost for different modelling schemes is shown in Table 2. As can be expected, globally fine mesh is able to faithfully predict the material behaviors, but huge amount of computational time is required as well. In contrast, if the A-FNM is applied, only elements within the refinement zone are converted to the refined configurations, the overall refined mesh is avoided and the computational time is saved by up to 47%, as shown in Table 2. Meanwhile, the high stress gradient can also be correctly captured by the moving local refinement, which ensures an accurate prediction for the delamination propagation.

Therefore, based on the previous discussions, both efficiency and accuracy are achieved by employing the A-FNM in the numerical modelling.

### 3.2 End notch flexure (ENF) test: mode-II delamination

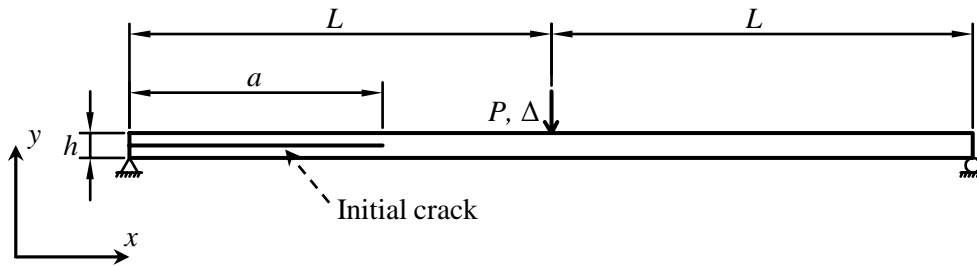


Figure 7: ENF test, set-up and loading conditions.

As shown in Fig. 7, the ENF mode II fracture problem reported in [9] is studied. The dimensions of the beam are length  $2L = 100\text{mm}$ , thickness  $h = 3\text{mm}$  and width  $1\text{mm}$ . An initial crack of length  $a = 30\text{mm}$  is embedded in the beam. The material properties used in the simulations are listed in Table 1. The prescribed displacement  $\Delta$  is applied at the center of the beam. The results are shown in the following.

Mesh size (mm)	5	1	A-FNM 5-1
Computational time (s)	23.2	29.09	24.47

Table 3: ENF test, computational cost for different models.

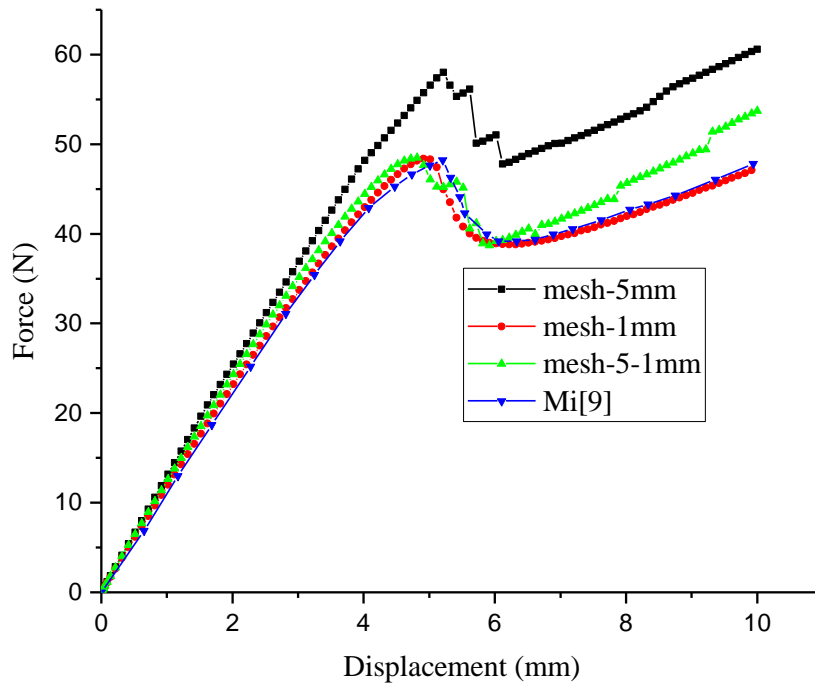


Figure 8: ENF test, comparison between traditional FEM models and A-FNM models.

### 3.3 Mixed-mode bending (MMB) test: mixed-mode delamination

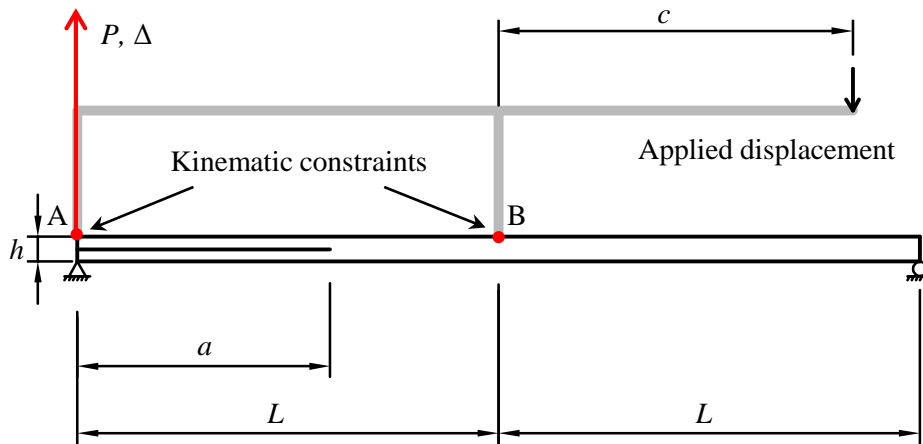


Figure 9: MMB test, set-up and loading conditions.

As shown in Fig. 9, the mixed-mode fracture problem reported in [9] is studied. The dimensions of the beam are length  $2L = 100\text{mm}$ , thickness  $h = 3\text{mm}$  and width  $1\text{mm}$ . An initial crack of length  $a = 30\text{mm}$  is embedded in the beam and the material properties used in the simulations are listed in Table 1. The prescribed displacement is applied at the right end of the rigid lever (with  $c = 41.5\text{mm}$ ). The left point A of the lever is connected to the beam through a hinge connection, while the point B can slide freely on the center of the beam. The displacement  $\Delta$  and force  $P$  at point A are measured for the loading response curves. The results are shown in the following.

Mesh size (mm)	3	1	A-FNM 3-1
Computational time (s)	16.99	45.92	19.89

Table 4: MMB test, computational cost for different models.

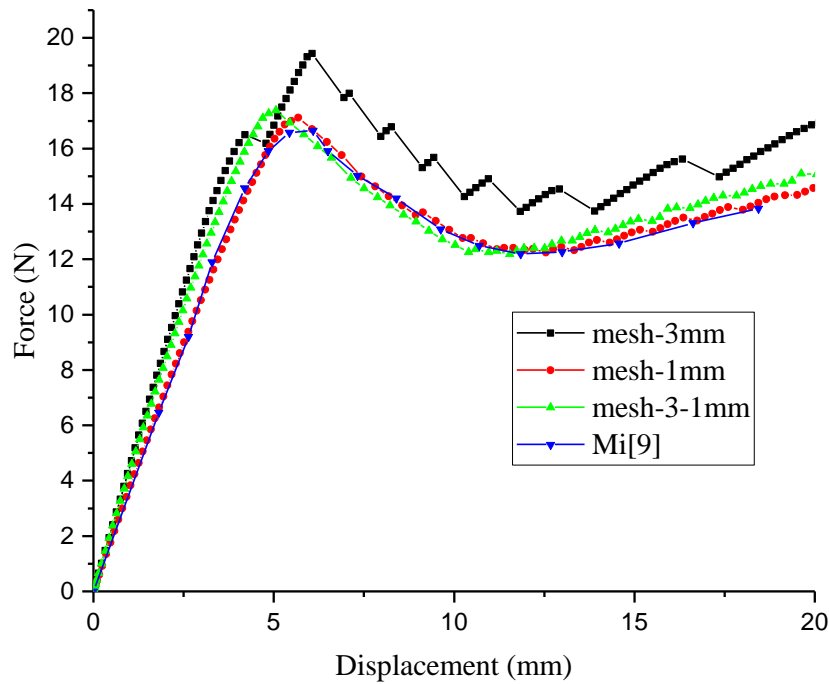


Figure 10: MMB test, comparison between traditional FEM models and A-FNM models.

#### 4 CONCLUSIONS

This paper presents a novel and efficient finite element (FE) technique for modelling delamination in laminated composites materials. The proposed adaptive floating node method (A-FNM) is able to deal with excessive mesh size requirement of the cohesive element (CE), and hence significantly reduces the computational cost.

An adaptive floating node element (A-FNE) with several elemental configurations is developed, namely, the master element, refined element and coarsened element. Based on the cohesive zone model, a refinement zone ahead of the crack tip is defined, such that the A-FNE within this zone should be transformed into the refined configuration to capture the highly nonlinear failure process. While, outside the refinement zone, a relatively coarse master element can be adopted to simply describe the smooth material behaviors. In this sense, by altering these prescribed element configurations adaptively with the damage evolution, local elemental refinement and coarsening schemes are performed.

Several numerical examples, including mode I, mode II and mixed-mode loading scenarios, are provided to demonstrate the performance of A-FNM. As shown in the previous chapter, both efficiency and the accuracy can be achieved by adopting the A-FNM in modelling delamination of composite laminates. The proposed A-FNM can also be easily applied to simulating other cohesive cracking problems, given the properly designed A-FNEs and the associated transformation criteria. The computational time will be reduced while accurate predictions can still be guaranteed.

#### ACKNOWLEDGEMENTS

The first author greatly acknowledges the research scholarship and research grant (No. R265000523646) from National University of Singapore.

## REFERENCES

- [1] B.Y. Chen, S.T. Pinho, N.V. De Carvalho, P.M. Baiz, T.E. Tay, A floating node method for the modelling of discontinuities in composites, *Engng. Fract. Mech.*, 127 (2014) 104-134.
- [2] B.Y. Chen, T.E. Tay, S.T. Pinho, V.B.C. Tan, Modelling the tensile failure of composites with the floating node method, *Comput. Methods Appl. Mech. Eng.*, 308 (2016) 414-442.
- [3] K. Song, Y. Li, C.A. Rose, Continuum damage mechanics models for the analysis of progressive failure in open-hole tension laminates, in: 52nd AIAA/ASME/ASCE/AHS/ASC Structures, Structural Dynamics and Materials Conference, 2011, pp. 1861.
- [4] B.Y. Chen, T.E. Tay, P.M. Baiz, S.T. Pinho, Numerical analysis of size effects on open-hole tensile composite laminates, *Compos. Part A Appl. Sci. Manuf.*, 47 (2013) 52-62.
- [5] N.V. De Carvalho, B.Y. Chen, S.T. Pinho, J.G. Ratcliffe, P.M. Baiz, T.E. Tay, Modeling delamination migration in cross-ply tape laminates, *Compos. Part A Appl. Sci. Manuf.*, 71 (2015) 192-203.
- [6] P.W. Harper, S.R. Hallett, Cohesive zone length in numerical simulations of composite delamination, *Engng. Fract. Mech.*, 75 (2008) 4774-4792.
- [7] A. Soto, E.V. González, P. Maimí, A. Turon, J.R.S. de Aja, F.M. de la Escalera, Cohesive zone length of orthotropic materials undergoing delamination, *Engng. Fract. Mech.*, 159 (2016) 174-188.
- [8] A. Turon, C.G. Davila, P.P. Camanho, J. Costa, An engineering solution for mesh size effects in the simulation of delamination using cohesive zone models, *Engng. Fract. Mech.*, 74 (2007) 1665-1682.
- [9] Y. Mi, M.A. Crisfield, G.A.O. Davies, H.B. Hellweg, Progressive delamination using interface elements, *J. Compos. Mater.*, 32 (1998) 1246-1272.
- [10] G. Alfano, M.A. Crisfield, Finite element interface models for the delamination analysis of laminated composites: mechanical and computational issues, *Int. J. Numer. Meth. Engng.*, 50 (2001) 1701-1736.